Mapping sugarcane globally at 10 m resolution using GEDI and Sentinel-2

Stefania Di Tommaso[1], Sherrie Wang[2], Rob Strey[3], and David B. Lobell[1]

[1]Department of Earth System Science & Center on Food Security and the Environment, Stanford University, USA
[2]Department of Mechanical Engineering & Institute for Data, Systems, and Society, MIT, USA
[3]Progressive Environmental & Agricultural Technologies, 10435 Berlin, Germany

Correspondence: David B. Lobell (dlobell@stanford.edu)

1   **Abstract.** Sugarcane is an important source of food, biofuel, and farmer income in many countries. At the same time, sugarcane
2   is implicated in many social and environmental challenges, including water scarcity and nutrient pollution. Currently, few of the
3   top sugar-producing countries generate reliable maps of where sugarcane is cultivated. To fill this gap, we introduce a dataset
4   of detailed sugarcane maps for the top 13 producing countries in the world, comprising nearly 90% of global production.
5   Maps were generated for the 2019-2022 period by combining data from the Global Ecosystem Dynamics Investigation (GEDI)
6   and Sentinel-2 (S2). GEDI data were used to provide training data on where tall and short crops were growing each month,
7   while S2 features were used to map tall crops for all cropland pixels each month. Sugarcane was then identified by leveraging
8   the fact that among all non-tree species grown in cropland areas, sugarcane is typically tall for the largest fraction of time.
9   Comparisons with field data, pre-existing maps, and official government statistics all indicated high precision and recall of our
10 maps. Agreement with field data at the pixel level exceeded 80% in most countries, and sub-national sugarcane areas from our
11 maps were consistent with government statistics. Exceptions appeared mainly due to problems in underlying cropland masks,
12 or to under-reporting of sugarcane area by governments. The final maps should be useful in studying the various impacts of
13 sugarcane cultivation and producing maps of related outcomes such as sugarcane yields.

1   Introduction

15 Sugarcane cultivation represents an important economic activity in many regions of the world, and serves as a substantial source
16 of food, beverage, and biofuel production. Roughly one-quarter of all ethanol production worldwide comes from sugarcane
17 (OECD et al., 2023), with many countries aiming to rapidly increase sugar ethanol production to meet energy independence
18 and climate mitigation goals. For example, the Organisation for Economic Co-operation and Development (OECD) and the
19 Food and Agricultural Organization (FAO) project that ethanol demand over the next decade will increase by 37% in Brazil and
20 107% in India (OECD et al., 2023), both countries where sugarcane is the primary feedstock. Moreover, millions of livelihoods
21 are derived from sugarcane production and processing activities, with some estimates putting the total number of livelihoods
22 dependent on sugarcane as high as 100 million (Jenkins et al., 2015).
23   Despite its contribution to food and energy security and economic growth, sugarcane cultivation has also been associated
24 with myriad challenges, including but not limited to large consumption of available freshwater and fertile cropland (Lee et al.,

2020), pollution of soils and ecosystems with nutrients and other chemical runoff (Allan et al., 2017), and exploitative labor conditions (El Chami et al., 2020). In addition, sugarcane receives a disproportionate amount of policy support in many countries through mechanisms such as market price support, ethanol mandates, and assistance to sugar mills. According to recent OECD estimates, sugar subsidies represent more than 20% of farm receipts globally, higher than any other food commodity (OECD, 2023). In some countries, this share is much higher, such as Mexico (37%), the United States (48%), Indonesia (55%), and the Philippines (62%) (OECD, 2023).

Despite the prominent role of sugarcane in many economies and the key support from government, few countries provide timely information on the status and dynamics of sugar cultivation. Such information could be helpful in studying the full effects of sugar cultivation on the health of both humans and the environment, thus informing public policy. Better data could also help aid sugar producers in their attempts to optimize productivity and profits, for example by helping to better understand factors that determine yield variation.

In an effort to fill the significant data gaps relating to sugarcane cultivation, we present here an approach and dataset that uses satellite remote sensing to map precise locations of sugarcane canopies around the world. Remote sensing has long been used to map areas of individual crops, with several countries producing annual, publicly available maps of crop types based on satellite data, such as the Cropland Data Layer (CDL) in the United States (Boryan et al., 2011) and the Annual Crop Inventory in Canada (Agriculture and Agri-Food Canada). Yet these maps have historically required ground data to calibrate the satellite models each year, which precludes their use in countries without a concerted government effort to maintain ground data collection.

Rather than rely on ground data, our approach relies on two features of sugarcane that together make it a unique crop throughout most of the regions where it is grown – it is much taller than most crops (often exceeding 3 meters in height), and grows across multiple years. In recent work (Di Tommaso et al., 2021, 2023), we demonstrated the ability of lidar measurements acquired by the Global Ecosystem Dynamics Investigation (GEDI) (Dubayah et al., 2020) to identify tall canopies within agricultural landscapes. Here we extend that work to map tall crops in each month over a four year period, and then identify sugarcane fields as those that are tall for a sufficiently large fraction of the study period. We find that this approach is able to map sugarcane with impressive detail across a wide number of countries, using both government statistics and independent maps in some countries to evaluate our product.

2 Datasets

The datasets utilized in this study include:

1. Global Ecosystem Dynamics Investigation and Sentinel-2 Sensors: Data from the Global Ecosystem Dynamics Investigation (GEDI) and Sentinel-2 (S2) satellite sensors were employed for data acquisition. Pre-processing steps were taken to prepare these datasets for analysis.

2. Land Cover Products: Various land cover products were employed to delineate the cropped areas within the study area.

57 3. Calibration and Validation Datasets: Specific datasets were utilized for the calibration and validation of the sugarcane
58 maps generated in this study.

2.1 GEDI data

60 GEDI, a sensor mounted on the International Space Station (ISS), captures lidar waveforms within the latitudinal range of 51.6°
61 N to 51.6° S to analyze the Earth's surface in three dimensions. It is the first spaceborne lidar instrument specifically designed
62 for assessing vegetation structure (Dubayah et al., 2020). Equipped with three lasers emitting near-infrared light at 1064 nm
63 wavelength, GEDI features two full-power lasers along with a third laser divided into dual beams, generating a total of four
64 beams. Through optical dithering across-track, each beam creates eight ground tracks (comprising four full-power tracks and
65 four cover tracks) spaced 600 meters apart on the ground. The shots produced have an average footprint diameter of 25 meters
66 and are separated by 60 meters along-track.

67 For this study, we used the GEDI dataset Level 2A (L2A) and Level 2B (L2B) from April 2019 to December 2022, available
68 in GEE data catalog.

69 The Level 2 data offer insights into the vertical canopy distribution derived from waveform returns at the footprint level. Our
70 primary dataset was GEDI's L2A Geolocated Elevation and Height Metrics Product, primarily comprising Relative Height
71 (RH) metrics. These RH metrics collectively characterize the waveform data acquired by GEDI, providing information about
72 the height at which a specific percentage of energy is returned relative to the ground. RH values are reported at 1% intervals,
73 resulting in a total of 101 metrics. Additionally, we used the L2B dataset to extract the GEDI view angle at each shot location,
74 specifically using the 'local beam elevation' property. This information was used to filter out GEDI shots with a view angle
75 below 1.51 rad, approximately 86.5 degrees, to avoid classification errors, as recommended in Di Tommaso et al. (2023).

76 The GEDI L2A dataset (`LARSE/GEDI/GEDI02_A_002_MONTHLY`) and L2B dataset (`LARSE/GEDI/GEDI02_B_002_MONTHLY`)
77 represent a rasterized version of the original GEDI products, where each GEDI shot footprint is depicted by a 25-meter pixel
78 (Healey et al., 2020). This rasterization process, however, may introduce an additional geolocation error beyond the initial
79 GEDI shot error. The raster images are structured as monthly composites of individual orbits conducted during the respective
80 month (refer to Figure 1). Within these raster images, RH values, along with quality flags and metadata, are preserved as raster
81 bands.

2.2 Sentinel-2

83 We employed the S2 surface reflectance harmonized collection, which is readily available in the Google Earth Engine (GEE)
84 platform. Clouds were filtered out using the S2 Cloud Probability dataset provided by SentinelHub in GEE, setting the max-
85 imum cloud threshold to 65%. Utilizing this dataset, we generated yearly (January to December) time series for each pixel.
86 These time series were then utilized to compute harmonic features, with an order of n=3 and omega=1, for a combination
87 of bands including 'NIR' (Near Infrared), 'SWIR1' (Shortwave Infrared 1), 'SWIR2' (Shortwave Infrared 2), 'RDED4' (Red
88 Edge Band 4), and 'GCVI' (Green Chlorophyll Vegetation Index) (Gitelson et al., 2005). This approach, proven successful in
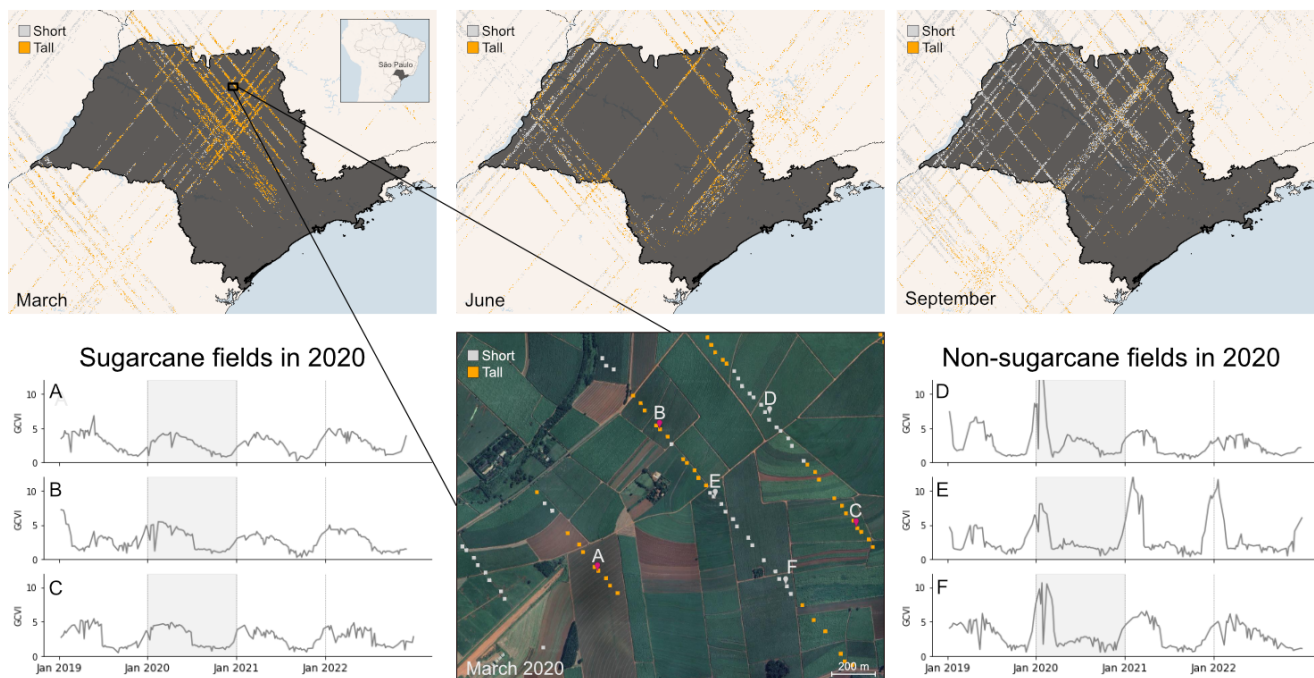
Figure 1. GEDI shots over São Paulo, the main sugarcane-producing state in Brazil. Top panel shows GEDI coverage in three different months, March, June and September, over the 4 years of data. Shots represented by a 25 m pixel are color-coded according to the short/tall classification by the GEDI model. Gaps in GEDI shot orbits may be attributed to quality issues. For instance, in June 2020, a significant portion of shots experienced low view angles and were subsequently filtered out, resulting in sparser GEDI coverage during this period, as illustrated in the top-middle panel. Additionally, in this region, there appears to be a higher proportion of shots classified as tall around the beginning of the year compared to later months. Bottom-middle panel show a zoom in at field level (© Google Earth Engine). GCVI S2 time series from 2019 to 2022 over sugarcane (on the left) and non-sugarcane fields (on the right), with the year 2020 highlighted in gray shading. GEDI accurately identifies tall fields that are growing sugarcane in March (A,B,C), and short fields that are not growing sugarcane in 2020 (D,E,F).

89 previous studies, has demonstrated efficacy in tasks related to crop type classification. GCVI is computed as

90 $\text{GCVI} = \text{NIR}/\text{Green} - 1$

91 For each spectral band or vegetation index $f(t)$, the harmonic regression takes the form

92 $$f(t) = c + \sum_{k=1}^{n} [a_k \cos(2\pi\omega kt) + b_k \sin(2\pi\omega kt)]$$

93 where a_k are cosine coefficients, b_k are sine coefficients, and c is the intercept term. The independent variable t represents
94 the time an image is taken within a year expressed as a fraction between 0 and 1. The number of harmonic terms n and the
95 periodicity of the harmonic basis controlled by ω are hyperparameters of the regression. This resulted in seven features per
96 band, for a total of 35 coefficients. These estimated values represent the S2-based harmonic features used in the subsequent
97 classification process.

2.3 Crop mask

99 Despite the abundance of global and regional cropland maps, considerable uncertainties and discrepancies persist regarding
100 both the total area and spatial distribution. To identify cropped areas comprehensively, we conducted an analysis encompassing
101 all global land cover products detailed in Kerner et al. (2023). Through visual inspection and subsequent examination of the
102 datasets outlined later, we observed that relying solely on a single product often resulted in the underestimation of cropland
103 area in certain regions, while another product exhibited similar limitations elsewhere. Recognizing the inherent risk of inac-
104 curate crop masks leading to either over- or underestimation, we opted to ensure a more robust global coverage by integrating
105 information from three distinct global land cover products. We defined a pixel as cropland if any of the three maps classified it
106 as such. This approach, involving the combination of these datasets, enabled us to enhance the completeness of cropland areas
107 worldwide.

108 The three global products are: the European Space Agency (ESA) WorldCover 2020 (Zanaga et al., 2021), ESRI 2020 global
109 Land Use Land Cover (Karra et al., 2021) and the 2019 GLAD Global Cropland Maps (Potapov et al., 2022).

110 A visual example of the three crop masks is provided for Brazil in Figure 2.

111 The ESA and ESRI 2020 products provide a global land cover map for 2020 at 10 m resolution, the former based on
112 Sentinel-1 and Sentinel-2 data, and the latter based on Sentinel-2 alone. Maps are available in the Google Earth Engine (GEE)
113 (Gorelick et al., 2017) official and community data catalogs, respectively (Roy et al., 2024). The 2019 GLAD Map provides
114 binary cropland classifications at 30 m. Classification is performed using bagged decision trees with features extracted from
115 time series of Landsat Analysis Ready Data (ARD).

116 Divergences exist among these land cover and land use products regarding the categorization of croplands, particularly
117 concerning the inclusion of tree crops. ESA WorldCover encountered issues such as underestimation of cropland areas in Brazil
118 and Africa, particularly in fragmented regions with mixed land covers. Contrarily, the WorldCover 2020 product identified more
119 tree cover, representing orchards, compared to other ESRI products.
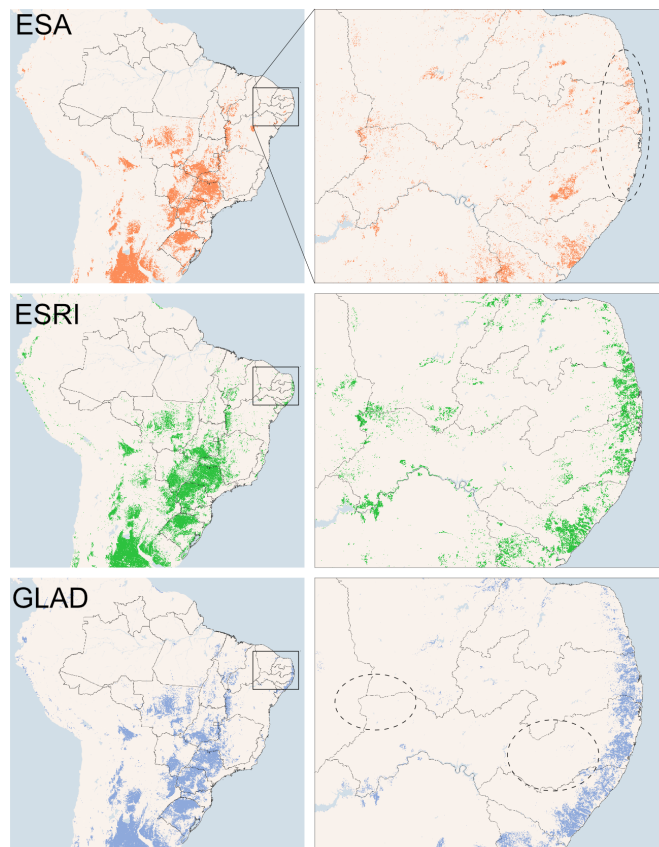
Figure 2. An example of difference in crop masks in Brazil (© Google Earth Engine). Dotted circles highlight areas of disagreement between maps. The ESA crop mask exhibits omissions in cropland detection in North-Eastern Brazil, whereas ESRI and GLAD capture more cropland in this region. ESRI tends to overmap cropland, often including orchards, while GLAD exhibits a more conservative approach, albeit missing some cropland in areas where both ESA and ESRI map it.

120   ESA's definition of cropland encompasses land that is covered with annual crops sowed and harvested at least once within
121   12 months after the sowing date. This cropland typically produces an herbaceous cover and may include some tree or woody
122   vegetation but excludes perennial woody crops. ESRI defines croplands as human-planted cereals, grasses, and crops not at tree
123   height, including rice paddies and irrigated agriculture, while GLAD excludes perennial woody crops and permanent pastures
124   from its definition, focusing on herbaceous crops for human consumption, forage, and biofuel.

125   **2.4   Calibration and Validation datasets**

126   Below we describe the datasets used for calibrating and validating the sugarcane maps. The data pertain to the main sugarcane-
127   producing countries according to the Food and Agriculture Organization (FAO) (Food and Agriculture Organization's Statis-

128 tical Database (FAOSTAT)), as presented in Table 1. Within each section, the countries are in decreasing order of sugarcane
129 production.

Table 1. Main sugarcane-producing countries according to FAO 2022.

Rank	Country	Production (million tonnes)	Production (%)	Area harvested (million hectares)	Area harvested (%)
1	Brazil	724	37.7	9.9	37.8
2	India	439	22.9	5.2	19.8
3	China	103	5.4	1.3	5.0
4	Thailand	92	4.8	1.5	5.8
5	Pakistan	87	4.6	1.3	5.1
6	Mexico	55	2.9	0.8	3.1
7	Colombia	35	1.8	0.4	1.4
8	Indonesia	32	1.7	0.5	1.9
9	USA	31	1.6	0.4	1.4
10	Australia	28	1.5	0.3	1.3
11	Guatemala	26	1.4	0.2	0.9
12	Philippines	23	1.2	0.4	1.5
13	South Africa	17	0.9	0.3	1.0
	Rest of the world	224	11.7	3.6	13.9

130 The list includes field-level labels, raster datasets, and government-reported sugarcane area data at administrative level 2 or
131 3. The specific sources for these datasets may vary depending on the region and the year of data collection. A summary of all
132 data available by region is provided in Table 2.

2.4.1 Point level data

134 The WorldCereal "sv_croptype_validations" dataset (Lesiv et al., 2023) includes observations of crop types in 2021 and 2022
135 at global scale along with their coordinates. This dataset was compiled and released by WorldCereal through a meticu-
136 lous process involving expert manual labeling. Utilizing an IIASA tool known as "Street Imagery validation" (accessible at
137 https://svweb.cloud.geo-wiki.org/), contributors were able to examine street-level images, including those from platforms like
138 Google Street View and Mapillary, and accurately identify crop types. It's important to note that this dataset is entirely distinct
139 and separate from existing maps and reference datasets, providing an independent source of valuable information for agri-
140 cultural analysis. The dataset contains labels for various crop types, including sugarcane, for several countries of interest. In
141 Brazil, sugarcane is the most prevalent crop label, accounting for 1.6k labels, followed by maize (~910) and soybean (~550).
142 In Mexico crop labels alongside sugarcane (50 labels) include maize (~40). Australia's crop distribution includes wheat (~120
143 labels) and sugarcane (~20). Meanwhile, in the Philippines, rice (~80 labels) is prevalent alongside sugarcane (~70).

Table 2. Summary of all available dataset by country and data type. The datasets used for calibrating our method are marked with an asterisk. WorldCereal point data refer to the years 2021-2022.

Country	Raster	Field points	Government statistics
Brazil	(binary) 2018-2019	World Cereal*	2022
India		Plantix 2020-2021* World Cereal	2019-2020
China	(binary) 2019-2020*	World Cereal	2022
Thailand		GSV points 2022* World Cereal	2022
Pakistan		World Cereal	2021-2022
Mexico		World Cereal*	2022
Colombia		World Cereal	2019
Indonesia			2021
USA	CDL 2019-2022*		2018
Australia		World Cereal*	2020-2021
Guatemala			2003
Philippines		World Cereal*	2021
South Africa	SANLC 2020*	SANLC points 2020 World Cereal	2017

144   Other countries represented in the WorldCereal dataset with a smaller number of samples include China, Colombia, India,
145   Pakistan, South Africa and Thailand.

146   In India we accessed crop type labels crowdsourced from farmers via Plantix, a free Android application developed by
147   Progressive Environmental and Agricultural Technologies (PEAT). The Plantix app is used by farmers who upload photos of
148   their crops to seek assistance in diagnosing and treating crop diseases. As part of the disease diagnosis process, PEAT uses
149   a convolutional neural network to assign crop labels based on the submitted photos. We used labels for the years 2020 and
150   2021 in the Indian states of Maharashtra and Uttar Pradesh (UP), where the accuracy of Plantix crop type labels exceeds 90%
151   for most major crops. Data have been cleaned to remove location inaccuracy (keeping only submissions with GPS accuracy
152   better than 10 m), as suggested by previous work by Wang et al. (2020). Additionally, to mitigate any bias, Plantix labels were
153   sampled to match the proportion of government-reported crop areas by crop, as certain labels, such as those for vegetables,
154   were more prevalent due to their susceptibility to diseases.

155   In Thailand we accessed crop type labels obtained with Google Street View (GSV) (Laguarta et al., 2023) for the year 2022.
156   These labels were generated by combining deep learning and street view imagery over Thailand, requiring minimal manual
157   labeling. Labels include sugarcane, cassava, maize, rice, and an "other" crop class. To ensure the labels were representative of
158   the landscape, they were sampled in alignment with government-reported crop areas.

159   In South Africa, independent reference points, used for validating the South African National land cover 2020 (SANLC

160   2020) map, are provided by the Department of Forestry, Fisheries and the Environment (South Africa - DFFE).

161   **2.4.2   Raster data**

162   In Brazil and China, sugarcane masks at 30m resolution were recently published by Zheng et al. (2022a) and Zheng et al.

163   (2022b). These maps were generated using a time-weighted dynamic time warping method. In Brazil, maps are available for

164   14 states for 2016–2019, with a reported overall accuracy for the year 2018 of 91%, and user's and producer's accuracies

165   reaching 94% and 87%, respectively. In China, maps are available for 2016–2020 for four southern provinces, which map over

166   over 95% of the sugarcane cultivation areas in China: Guangxi (64%), Yunnan (18%), Guangdong (12%), and Hainan (1%)

167   provinces. The reported overall accuracy for the year 2019 is 92.7%, with reported user's and producer's accuracies of 85.6%

168   and 86.7%.

169   The Cropland Data Layer (CDL) (Boryan et al., 2011) produced by the United States Department of Agriculture (USDA)

170   provides yearly crop type maps across the conterminous US at 30 m spatial resolution. Maps are based on Landsat and other

171   satellite imagery using training data from the Farm Service Agency (FSA). Sugarcane plantations in the contiguous United

172   States are primarily concentrated in three states: Florida, Louisiana, and Texas. Accuracy of CDL on FSA labels are available

173   in the CDL metadata, with precision and recall for sugarcane in 2019-2022 exceeding 72%, 94% and 93% in Texas, Florida,

174   and Louisiana, respectively.

175   The South African National Land Cover 2020 (SANLC 2020), recently published by the Department of Forestry, Fisheries,

176   and the Environment (South Africa - DFFE), was generated at a 20-meter resolution utilizing S2 imagery. The overall accuracy

177   of this land cover classification is 85.5%. The accuracy for the sugarcane classes surpasses 95% for user's accuracy and 82%

178   for producer's accuracy.

179   **2.4.3   Government statistics**

180   The Brazilian Institute of Geography and Statistics (IBGE) (Instituto Brasileiro de Geografia e Estatística) offers comprehen-

181   sive data on various agricultural metrics, including the planted and harvested areas, production volumes, and average yields, on

182   an annual basis for agricultural commodities. In our research, we utilized the municipality-level (admin 2) data for sugarcane

183   planted and harvested areas for the latest available year, 2022.

184   In India, the Ministry Of Agriculture and Farmers Welfare releases crop production statistics (Indian Department of Agri-

185   culture) at the district level (admin 2). For our analysis, we incorporated district-level crop area statistics for the most recent

186   available year, which is the 2019–2020 growing season.

187   In China, the Statistical Yearbooks serve as annual publications providing comprehensive insights into the economic and

188   social development of each province. These publications encompass data from the previous year, offering statistics at both

189   the provincial level and the local levels of cities (level 2). For our analysis, we obtained sugarcane sown area data from the

190   Statistical Yearbook for the 2022 growing season for the four sugarcane producing provinces: Guangdong (Guangdong Provin-

191 cial Bureau of Statistics), Guangxi (Statistics Bureau of Guangxi Zhuang Autonomous Region), Yunnan (Yunnan Provincial

192 Bureau of Statistics), and Hainan (Hainan Provincial Bureau of Statistics).

193   The agricultural statistics of Thailand for the year 2022, including data on sugarcane harvested area, were sourced from the

194 relevant government authority at province level (admin 1) (Office of Agricultural Economics).

195   The district-wise statistics on crops area and production for the growing season 2021-22 in Pakistan were obtained from

196 the government of Pakistan at district level (admin 3) (Ministry of National Food Security and Research). Due to uncertainties

197 regarding district borders over time, the data were processed and aggregated at level 2 to ensure consistency and accuracy in

198 the analysis.

199   The annual agricultural statistics provided by the Government of Mexico (Agri-Food And Fisheries Information Service)

200 encompass a wide range of information, including data on planted area, harvested area, damaged area, average rural prices,

201 volume, and value of production for both cyclical and perennial crops, categorized by water modality. These reports cover all

202 32 federal entities of the country, with detailed breakdowns at the national, state, district, and municipal levels (admin 2). For

203 our analysis, we specifically extracted sugarcane area data at the municipality level for the year 2022.

204   The National Agricultural and Livestock Survey Survey (ENA) conducted in 2019 (National Administrative Statistics De-

205 partment), provides data on sugarcane planted area, production, and yield by region (admin 1) for the year 2019 in Colombia.

206   The Indonesia Central Statistics Agency (Badan Pusat Statistik (BPS)) serves as the official statistical agency of the Indone-

207 sian government, tasked with collecting, processing, analyzing, and disseminating statistical data and information throughout

208 the nation. It provides comprehensive statistics on plantation area by province (admin 1), which offers insights into the distri-

209 bution of agricultural land across different regions of Indonesia. Specifically, the dataset comprises the area of annual crops

210 such as oil palm, coconut, rubber, coffee, cocoa, and tea, representing the planted area at the end of the year. Additionally,

211 the dataset includes information on seasonal crops like tobacco and sugarcane, with data reported as the monthly cumulative

212 harvested area. The most recent report refers to the year 2021.

213   In the United States, county-level (admin 2) statistics on sugarcane area are available from the United States Department of

214 Agriculture's National Agricultural Statistics Service (NASS) (USDA Natlional Agricultural Statistics Service). We accessed

215 the most recent data for counties in the key sugarcane-producing states Florida, Louisiana, and Texas for the year 2018 using

216 the NASS Quickstats database.

217   Statistics on the production of agricultural commodities, encompassing cereal and broadacre crops, fruit and vegetables, and

218 livestock on Australian farms, are provided by the Australian government (Australian Bureau of Statistics). These statistics are

219 made available on a yearly basis, with the most recent data available for the 2020-2021 growing season (at Statistical Areas

220 Level 2).

221   In Guatemala, data on sugarcane production by department (admin 1) for the agricultural year 2002/2003 was obtained from

222 the IV National Agricultural Census (Guatemala Nationl Institue of Statistics). Sugarcane accounted for 28.4% of the total area

223 cultivated with permanent and semi-permanent crops. The department of Escuintla recorded the highest sugarcane productions

224 for the census year, comprising 87.7% of the total production.

The Philippine Statistics Authority (PSA) (Philippine Statistics Authority) releases annual provincial statistics on Agriculture and Fisheries. These statistics include the total area of sugarcane and the percent distribution of sugarcane production by region. Although direct access to sugarcane area by region is not available, an approximation can be made by assuming that the percentage of production falls within the same range as the percentage of area by region. The most recent year for which data is available is 2021.

The Statistics department of South Africa (Statistics Department - South Africa) conducts the Census of Commercial Agriculture, 2017 (CoCA 2017), which publishes results at the municipal level (admin 3). The primary objective of this survey is to gather financial, production, employment, and related information pertaining to the commercial agriculture industry in South Africa. It is important to note that CoCA 2017 only covers enterprises registered for value-added tax (VAT). Consequently, the census does not include smallholder farming. Instead, it utilizes VAT records as a sampling frame, thereby excluding entities that are non-VAT registered. It is noteworthy that commercial farmers account for 80% of the country's agricultural value.

3 Methods

3.1 Sugarcane phenology

Sugarcane is primarily grown in tropical and sub-tropical regions of the world. It is a tall semi-perennial crop, with a growth cycle lasting typically between 12 to 18 months before it is ready for harvesting. The specific duration of this cycle varies depending on factors like the sugarcane variety, local climate, and geographical conditions in each region. After the first harvest, sugarcane can regrow from the same root systems for multiple years (ratoon crops), resulting in subsequent yield losses due to a reduction in stalk population. To ensure sustainable yields and maintain soil fertility, sugarcane areas are often rotated with other crops to aid in nitrogen fixation for subsequent sugarcane growth seasons. Cultivation practices also involve planting different sugarcane varieties within the same plantations to minimize susceptibility to diseases. Figure 1 provides a visual example of sugarcane time series in Brazil and rotation with soybean.

3.2 Area of interest

We initiated our study by focusing on the main sugarcane-producing countries listed in Table 1.

We established a $2° \times 2°$ grid overlaying these countries. To reduce computation, grid cells were selected based on two criteria: a cropland coverage exceeding 1%, determined using the European Space Agency (ESA) Crop Mask dataset, and a sugarcane area greater than 0, derived from the Spatial Production Allocation Model (SPAM) (International Food Policy Research Institute, 2019). These selected grid cells represent the regions where we aimed to predict sugarcane presence.

3.3 GEDI data processing

All GEDI shots from April 2019 to December 2022 over cropland pixels, passing over these $2° \times 2°$ grid cells, were classified as either short, tall, or tree by a GEDI model trained in Di Tommaso et al. (2023). This model is trained on high-accuracy crop

255 type labels from three regions. The tall class is represented by maize samples, and the short class is a mix of mostly soybeans,
256 rice and spring barley labels. Each classification was accompanied by a confidence value.

257   Prior to further analysis, the predicted shots underwent a filtering process to retain only high-quality data. Initially, shots
258 were filtered based on the quality and degrade flags provided as properties in the GEDI dataset. Additionally, predictions with
259 confidence scores lower than 0.8 were discarded. A crucial step involved filtering out shots with low view angles and those
260 over high-slope terrain, defined as areas with slopes exceeding $5°$, as both factors can impact the accuracy of GEDI model
261 predictions. View angle information was retrieved from the L2B dataset, enabling the exclusion of low view angle shots.

262   Furthermore, we opted to exclude shots identified as belonging to the tree class by the GEDI model. This decision was
263 motivated by the likelihood that such shots may encompass a mixture of crops and trees within the GEDI footprint, which, at
264 a diameter of 25 meters, surpasses the size of the 10-meter S2 pixel by over four times.

265   Figure 1 shows the spatial coverage of GEDI over time and the changing proportion of tall and short labels over cropland.

266 ### 3.4 S2 model training and classification

267 Utilizing the GEDI predictions as binary labels, we trained separate local S2 models for each grid cell and for each month
268 of the year. We opted for a random forest model for its well-documented advantages, including high accuracy, computational
269 efficiency, and smooth integration into large-scale applications within GEE. The S2 models were trained using S2 harmonics
270 coefficients as features and the GEDI predictions as labels. For each grid cell, we aggregated GEDI labels for each month across
271 different years and extracted the corresponding S2 features for the same year as the GEDI label. Subsequently, we constructed
272 pooled models for each month and generated predictions for four years, utilizing features specific to each year. This process
273 yielded 48 monthly predictions for each grid cell, where each 10 m by 10 m pixel within the crop mask was classified as either
274 short or tall. Most of the grid cells have more than 9,400 GEDI training labels used for training the S2 model, with the 5th
275 percentile and 95th percentile of the number of training labels being 768 and 69,000 samples, respectively.

276   In order to reduce spatial artifacts that may arise during the process of mosaicking adjacent cells, we implemented a strategy
277 where we generated predictions for pixels within a $0.2°$ buffer around each cell. This buffer ensured that neighboring cells had
278 overlapping coverage. Subsequently, on a monthly basis, we performed the mosaicking process, selecting for the overlapping
279 regions the predictions from the cell with the higher GEDI-S2 kappa score. This ensured that the final mosaic maintained the
280 highest possible accuracy, enabling a smoother transition between adjacent regions.

281 ### 3.5 Calibration/Sugarcane identification

282 To distinguish sugarcane from other tall crops, such as maize, we computed the frequency of tall predictions for each pixel
283 across the 48 monthly predictions. Pixels were classified as sugarcane if the frequency of tall predictions exceeded a certain
284 threshold, based on the principle that sugarcane remains tall for longer periods of time compared to annual crops like maize.
285 However, using a single threshold across all countries is suboptimal, as the appropriate threshold depends on the mix of crops
286 alongside sugarcane, the phenological characteristics of both sugarcane and other crops, and local agricultural management
287 practices.

288   The selection of the threshold was guided by a calibration approach based on available *in situ* data. To determine the threshold

289   in countries where we had large number of labels of sugarcane and different crop type classes, we used point level calibration

290   and relied on the threshold that produced the highest kappa score.

291    $Kappa\ score = \dfrac{P_o - P_e}{1 - P_e}$

292   where

293   – P_o is the proportion of observed agreement, i.e. the accuracy achieved by the model

294   – P_e is the proportion of agreements expected by chance

295   This methodology was applied in Brazil, India, Thailand, and South Africa, where we had many (> 600) ground samples.,

296   as well as in China and the USA where point labels were unavailable but crop type maps developed through a combination

297   of ground and satellite data were accessible. In these cases, samples were obtained by random sampling of the reference crop

298   maps.

299   In other countries with a limited availability of sugarcane labels (n<200), we extracted at each location of a sugarcane

300   label the number of tall months in our map, and then calculated the 10th percentile of this value across all such locations.

301   This threshold therefore ensures that 90% of the reference sugarcane labels would be classified as sugarcane. In countries

302   where ground labels were lacking, we set the threshold equal to that of a nearby country, based on the assumption that the

303   characteristics of the sugarcane were most similar in nearby locations.

304 **3.6 Validation**

305   To validate our sugarcane maps, we compared them against a combination of available point samples, raster maps of crop

306   type, and reported sugarcane area of government statistics. Because of the nature of sugarcane, a semi-perennial crop, we are

307   mapping stable sugarcane area in the 4-year period. Although we do not expect perfect agreement against government reported

308   planted or harvested area for a single year, a comparison with government data still provides a useful assessment of how well

309   our maps capture broad spatial patterns.

310 **4 Results**

311   We first present the outcomes of the calibration strategy, outlining the optimal threshold for sugarcane identification based

312   on available data specific to each country. For validation purposes, we compare the results against field points and rasters

313   and assess the sugarcane area against government-reported data. These evaluations are conducted for each country using the

314   selected threshold and employing a combined ESA and GLAD crop mask. We find that combining these two maps helps cover

315   the majority of cropland in most regions while avoiding the mapping of orchards that are often included in the ESRI crop mask.

316   It's worth noting that even though validation results are provided for the cropland area mapped in the ESA and GLAD masks, a
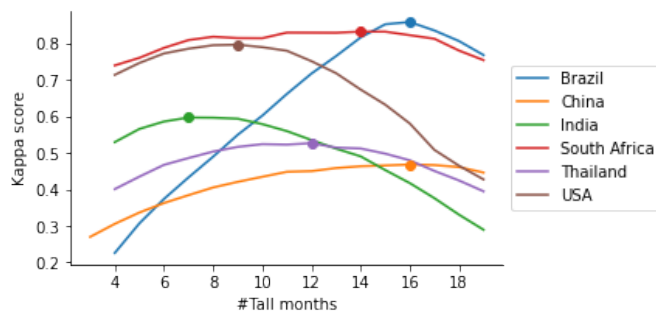
Figure 3. Identification of the threshold for classifying pixels as sugarcane based on the kappa score for countries with abundant in situ crop type labels. X-axis shows number of months (out of a total of 48) where a tall crop was present, and y-axis shows the kappa score for a model that classifies as sugarcane all pixels with at least this many months with tall crops. Dots represent the maximum kappa score value and the chosen threshold for each country. In India, 7 and 8 month thresholds were tied and we opted to use a threshold of 8 to be conservative and prioritizing higher precision in our map, avoiding the inclusion of other crops.

317 sugarcane map is produced for the area covered by the ESRI crop mask as well, and it is made available in our dataset. Further
318 details about the data release are provided in the data availability section.

4.1 Calibration

320 For calibration, we employed various strategies due to the absence of in situ labels across all countries of interest. Results of
321 the calibration for countries with abundant ground samples are illustrated in Figure 3.

322 China, Thailand, and South Africa exhibit low sensitivity to the chosen threshold. In Thailand, the threshold is optimized to
323 avoid mostly confusion with cassava, a shrubby perennial that is usually 2–3 m in height. In South Africa, most of the point
324 samples are sugarcane, followed by small-scale and commercial annual crops. The optimal threshold helps to avoid confusion
325 with commercial irrigated annual crops.

326 The threshold selection is critical in Brazil, mostly to avoid confusion with maize, another tall crop ranging from 1.2–4 m in
327 height.

328 India and the US exhibit moderate sensitivity and lower optimal thresholds, perhaps due to shorter sugarcane phenological
329 cycles and the absence of other crops that appear tall in sugarcane growing areas. In India, the calibration curve appears very
330 flat between 7 and 8 months. To err on the side of caution, and avoid including other crops in our sugarcane map, we chose
331 to set the threshold at 8 months. In the US, the threshold serves to avoid confusion with maize, which is present but not as
332 common as in Brazil.

333 In regions where insufficient labels were available for crop types other than sugarcane to compute a reliable kappa score, such
334 as Mexico, Australia, and the Philippines, we adopted the 10th percentile approach. Conversely, in regions where no data were
335 accessible, we determined the threshold based on the neighboring country. This last strategy was applied in Pakistan, Colombia,

336 Indonesia, and Guatemala. Results of the chosen calibration method and threshold for all the countries are summarized in Table
337 3.

Table 3. Summary of the thresholds used for calibrating the sugarcane maps. The threshold is expressed as the number of months over a 48 month-period. Diverse metrics and data sources have been adopted across different countries as a result of disparities of *in situ* data availability. Rows marked with N/A denote the absence of available data, and a threshold from a neighboring country was adopted. Specifically, Pakistan employed the same threshold as India, Colombia as Mexico, Indonesia as Thailand and Guatemala as Mexico. Threshold range from as low as 8 months in India, Pakistan and the Philippines, to as high as 16 months in Brazil and China. These disparities reflect differences in sugarcane phenology, management practices, and co-cultivation with other crops, tall or short.

Rank	Country	Data Source	Metric	Threshold
1	Brazil	WorldCereal	kappa	16
2	India	Plantix points	kappa	8
3	China	Raster	kappa	16
4	Thailand	GSV points	kappa	12
5	Pakistan	N/A		8
6	Mexico	WorldCereal	10th perc	14
7	Colombia	N/A		14
8	Indonesia	N/A		12
9	USA	CDL	kappa	9
10	Australia	WorldCereal	10th perc	11
11	Guatemala	N/A		14
12	Philippines	WorldCereal	10th perc	8
13	South Africa	SANLC points	kappa	14

338   Some regions may experience subnational variation in sugarcane cultivation practices. For instance, in India, where we have
339 a substantial number of Plantix samples, we observed some differences between the states of Maharashtra and Uttar Pradesh.
340 While the overall threshold for India is 8 months, the optimal thresholds are 9 months for Maharashtra and 7 months for
341 Uttar Pradesh. Unfortunately, in the current study, we lack the amount of data necessary to conduct such detailed analysis at a
342 subnational scale for all countries.

343 **4.2 Sugarcane Maps**

344 The sugarcane maps for the main producing countries, obtained applying the calibration threshold previously identified across
345 the 48 monthly predictions, are shown in Figure 4. These maps exhibit high quality, with no significant imprints from scene
346 borders or major artifacts, despite using separate S2 models for each grid cell. This indicates that the models from adjacent
347 grid cells are robust. Additionally, the buffering and subsequent monthly mosaicking processes contribute to creating an even
348 smoother and more cohesive map.
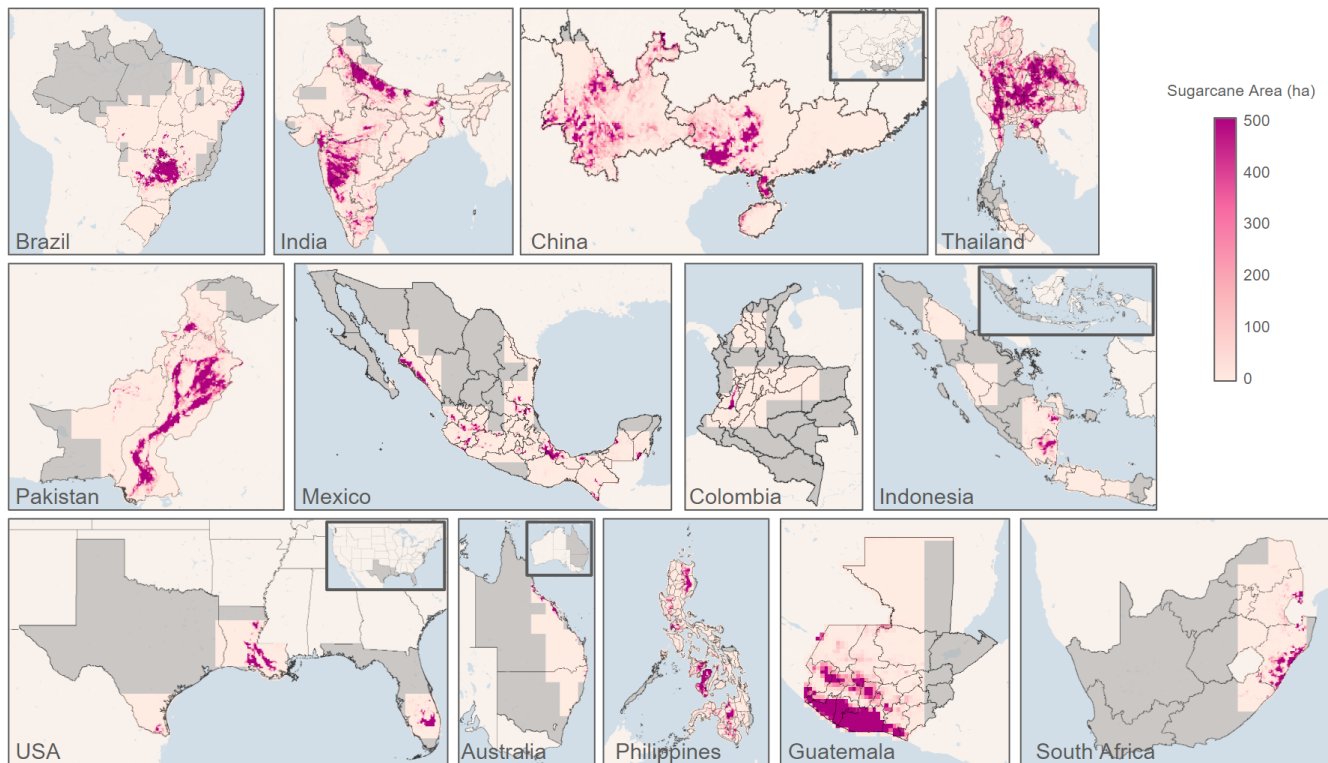
Figure 4. Sugarcane maps for top 13 producing countries (© Google Earth Engine). For visualization, the original 10 m maps were resampled at 10 km resolution and show the sugarcane area in hectares for each 10 × 10 km pixel (1000 ha). The area that we did not process–due to lack of cropland or sugarcane–is colored in gray. For China, Indonesia, the US, and Australia, the highlighted gray area in the inset indicates the regions for which zoom-ins are provided.

4.3 Validation

4.3.1 Validation against field points

We provide a summary of point-level validation results for the sugarcane maps by country based on field-level data in Figure 5.

Performance metrics vary across countries, with F1 scores for sugarcane exceeding 0.8 for most countries. Notably, Brazil, Mexico, Australia, the Philippines, and South Africa exhibit strong performance, with F1 scores higher than 0.9. However, exceptions are observed in certain regions.

In Thailand, utilizing GSV samples yields an F1 score on sugarcane of 0.57, with precision and recall scores of 0.53 and 0.62, respectively. The predominant confusion is observed with the cassava class. This is not surprising given their coexistence in similar geographic regions and that cassava plants can grow over 2 m. It is also common for farmers to alternate between cassava and sugarcane cultivation in their fields. In contrast, performance in Thailand using WorldCereal data appears to be
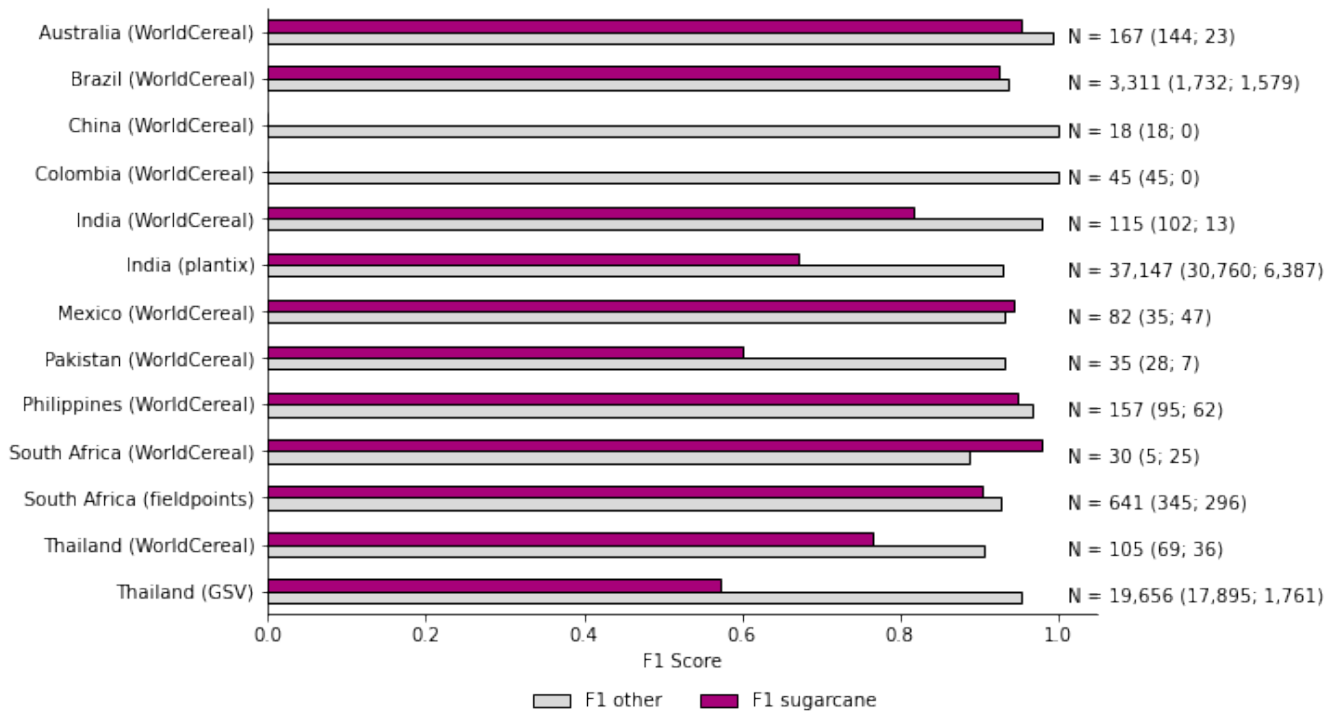
Figure 5. Results of point level validation. In parenthesis are reported the numbers of samples labeled non-sugarcane and sugarcane labels.

360 better, but it is essential to note that cassava is not included in this dataset. WorldCereal crop classes in Thailand include rice,

361 sugarcane, and maize. Additionally the number of WorldCereal samples (75) is substantially limited compared to GSV samples

362 (~19k).

363   In India, contrasting results are observed between different datasets. For instance, using Plantix labels yields an F1 score of

364 0.67 for sugarcane, with precision and recall at 0.65 and 0.69, respectively. Notably, performance in Maharashtra (MH) lags

365 behind Uttar Pradesh (UP), with F1 scores of 0.56 and 0.7, respectively. The lower performance of MH is mostly due to low

366 precision (0.5), caused from misclassification of maize as sugarcane. Conversely, utilizing WorldCereal data in India results

367 in an F1 score of 0.82 for sugarcane, with precision and recall metrics of 1 and 0.69, respectively. This is explained by fewer

368 maize labels, with labels for the other class including mostly rice and wheat. It's worth noting in this case as well the limited

369 number of WordCeral samples (115) in this region compared to Plantix (~37k).

370   Similarly, Pakistan, using WorldCereal labels, exhibits an F1 score of 0.6, primarily attributed to low recall (0.43).

4.3.2 Validation against raster datasets

372 We offer a visual comparison between reference maps and predicted sugarcane maps for regions where crop type maps are

373 available, depicted in Figure 6. In cases where multiple years of sugarcane maps were accessible but did not correspond to the
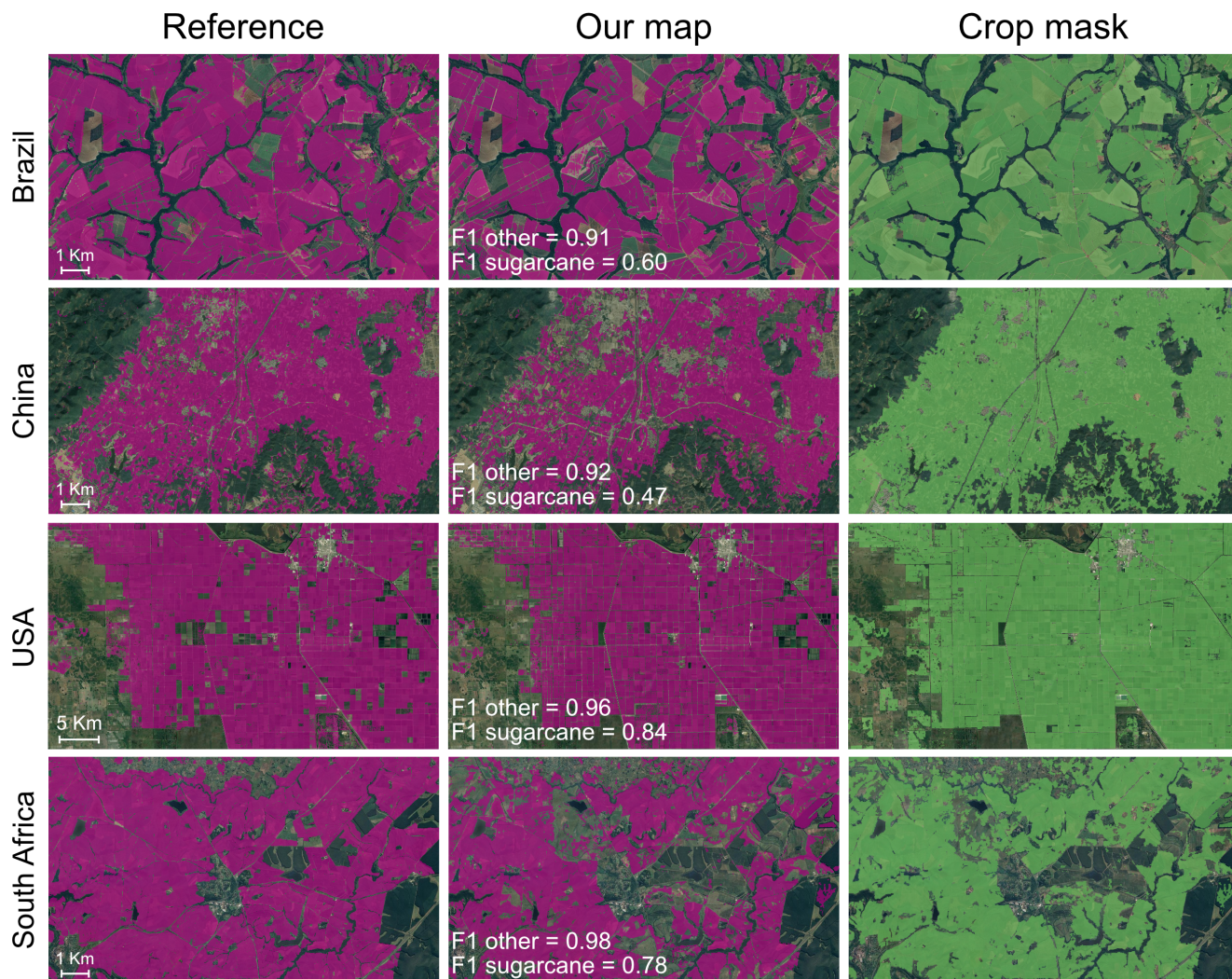
Figure 6. Comparison between our sugarcane maps and reference rasters. Maps show zoom-ins of key sugarcane-producing regions in Brazil, China, US and South Africa (© Google Earth Engine). The reported metrics pertain to the entire region covered by the reference maps, not just the illustrated portions. The absence of sugarcane in certain predicted maps for select regions can be attributed in part to the crop mask selection (ESA+GLAD), which omits certain cropped areas (e.g., South Africa).

374 same years as our study, as in the case of Brazil and China, we utilized the two most recent years. Sugarcane was classified
375 as present in a pixel if it appeared as sugarcane at any point during these years, accounting for potential crop rotation. For the
376 US, where the Cropland Data Layer (CDL) is available annually from 2019 to 2022, we considered a pixel as sugarcane if it is
377 classified as sugarcane for at least two years out of the four.

378 To evaluate a measure of agreement between maps, we randomly sampled 10k cropland points for each state/admin1 covered
379 by the raster maps and reported F1 scores in Fig. 6. These metrics pertain to the entire mapped raster area, not just the portion
380 depicted in the zoomed-in view in the figure. Across different regions, F1 scores for sugarcane varied, ranging from 0.47 in
381 China to 0.84 in the USA.

382 In Brazil, the raster encompasses 13 states, with a relatively lower F1 score of 0.6 for sugarcane. This discrepancy is reflected
383 in the precision of 0.55 and recall of 0.66. However, in São Paulo, the F1 score improves to 0.74, characterized by higher
384 precision (0.82) and recall (0.67).

385 In China, the overall F1 score of 0.47 is derived from data spanning all four provinces. Notably, in Guangxi, the primary
386 sugarcane-producing region, the F1 score increases to 0.64, with the same precision and recall (both 0.64).

387 In the USA, precision and recall values stand at 0.85 and 0.82, respectively, indicating strong agreement between maps.

388 Conversely, in South Africa, precision and recall are slightly lower at 0.73 and 0.84, respectively, with a portion of labels for
389 commercial annual crops misclassified as sugarcane.

4.3.3 Validation against government statistics

391 To evaluate the accuracy of our sugarcane maps, we conducted a comparison with government reported statistics on sugarcane
392 area. We present the results in Figure 7 at the finest available scale provided by the governments. The only exception is
393 Pakistan, where we group the data at level 2 due to uncertainties/changes of level 3 administrative division borders over time.
394 Only administrative regions fully covered by our sugarcane maps are included in these results. We find overall good agreement
395 with government statistics for the main sugarcane-producing areas. Many countries (6) exhibit an R^2 of 0.85 or higher (Brazil
396 0.92, Pakistan 0.85, USA 0.99, Australia 0.9, Guatemala 0.97, Philippines 0.85).

397 Some exceptions occur in regions where inaccurate crop masks lead to over prediction of sugarcane area. Specifically,
398 in Yunnan, China, many orchard areas are included in the crop mask, and because these are tall for the entire year tend to
399 get classified by our model as sugarcane. Moreover, regions predominantly characterized by (irrigated) maize cultivation, as
400 evident in Sinaloa, Mexico, also tend to be misclassified as sugarcane by our model, presumably because they are growing
401 maize every year of the study period. Outside of these problematic regions, the model agrees well with official statistics in each
402 country. The R^2 increases from 0.73 to 0.96 when removing Yunnan in China, and from 0.46 to 0.78 when removing Sinaloa
403 in Mexico.

404 Moving to the assessment of main sugarcane-producing states within each country, São Paulo emerges as the main con-
405 tributor to Brazil's sugarcane landscape, accounting for over half of the planted area. Here, our analysis demonstrates robust
406 agreement between predicted and government-reported sugarcane areas, with an R^2 value of 0.94 and a slope of 0.88, based
407 on 630 administrative units.

In India, Uttar Pradesh (UP) stands as the primary sugarcane producer, followed by Maharashtra and Karnataka, the three states together contribute approximately 80% of the nation's sugarcane production. Notably, UP exhibits strong agreement with government-reported data, with an R^2 value of 0.95 and a slope of 1.26. Conversely, while Maharashtra and Karnataka also demonstrate a good agreement, with R^2 values of 0.79 and 0.96, respectively, the regression line slopes for both states is close to 2 (2.2), suggesting that the predicted sugarcane area is more than twice the reported area.

In China, Guangxi has the highest cultivation land and production of sugarcane, accounting for more than 60% of the total national area. We observe strong agreement with the government-reported area, with R^2 value of 0.97 and a slope of 1. It is possible that in India, as in China, a source of our over prediction of sugarcane area is the underlying crop masks, which might include land uses other than arable crops such as permanent tree crops or bamboo.

In Colombia, agricultural statistics are reported at the administrative level 1, known as departments. Our map provides full coverage solely for the Caldas department, a minor sugarcane-producing region, with an estimated area three times smaller that the reported area. It's worth noting that the primary sugarcane-producing areas, Valle de Cauca and Cauca, are only partially covered by our maps. Despite this, we observe substantial agreement between the mapped areas and the government-reported sugarcane area.

In Indonesia, statistical data on sugarcane production is available at provincial level (admin 1). However, only Jawa Barat, a minor sugarcane-producing province, is fully covered by our sugarcane map, while the main sugarcane-producing provinces, such as Lampung and Sumatra Selatan, have partial coverage. Despite this limitation, our analysis reveals agreement between the reported sugarcane area and the mapped areas in these provinces.

In US, Florida and Louisiana are the main producers, with R^2 of 1 and 0.9, respectively. In Australia, Queensland serves as the primary producer state, demonstrating an R^2 value of 0.91.

Regarding South Africa, the available government statistics pertain exclusively to commercial farmers, whereas our analysis includes all sugarcane fields, encompassing both commercial and smallholder operations. Despite this disparity, we report the agreement because commercial farmers contribute to over 80% of the total sugarcane production in the country. The lower R^2 value may be attributed to the type of reported statistics as well as potential crop mask issues.

5 Discussion

5.1 Agreement with field data and raster

Synthesizing lessons from point and raster data, we find that GEDI and S2-based sugarcane mapping presents challenges, particularly in regions where tall crops like cassava and maize, especially irrigated maize, coexist with sugarcane. We also observe discrepancies in performance between point and raster data.

In Brazil, we observed lower performance in raster maps (F1 score of 0.6) compared to WorldCereal point data (F1 score of 0.9). This discrepancy could be attributed to the construction of reference rasters, wherein sugarcane is defined as the union of the two most recent years, along with differences in the years considered. In Guangxi, China, we observed similarly low
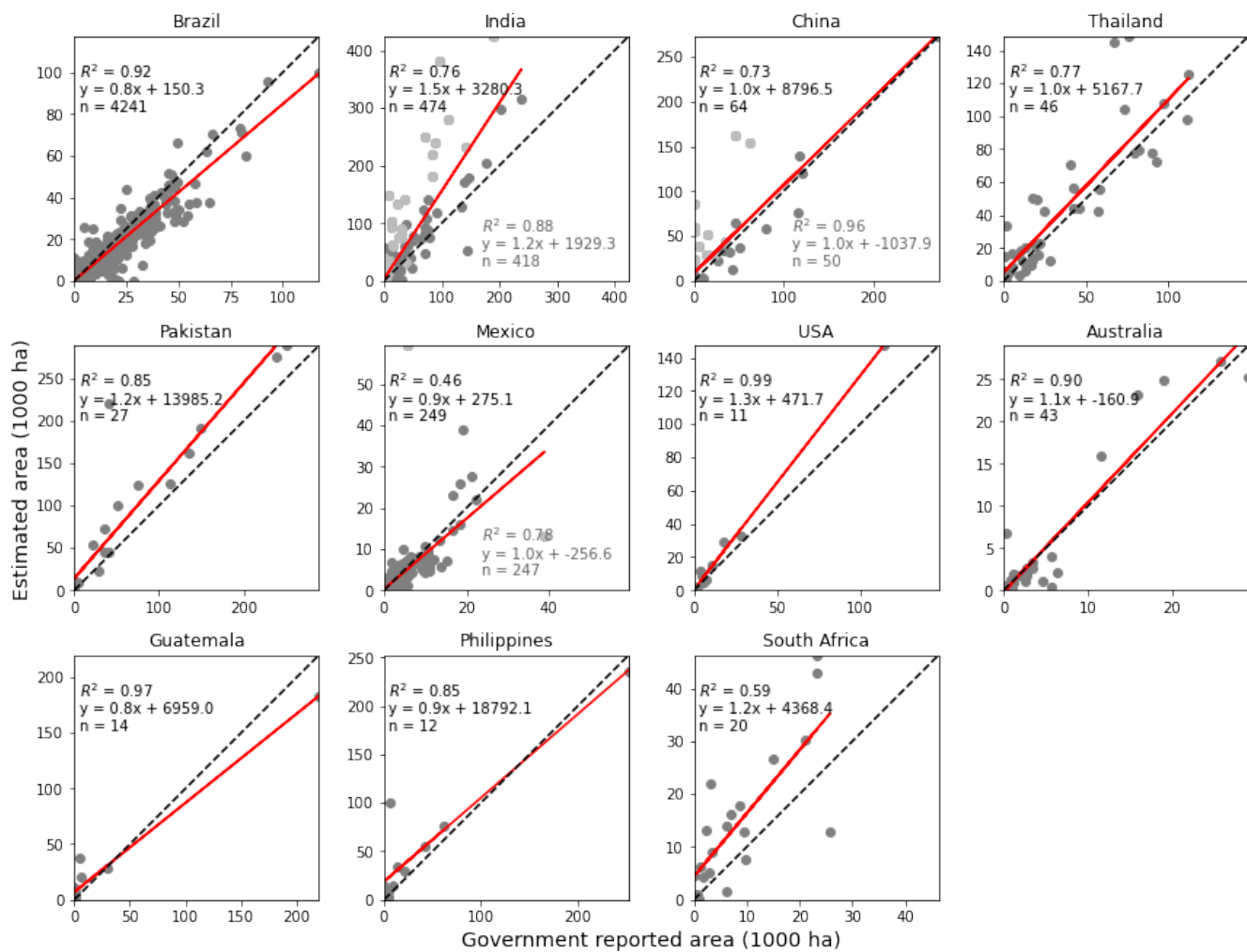
Figure 7. Comparison of the sugarcane area in our maps with government statistical data. On the top-left corner are reported the results using all data points. For some countries, on the bottom-right are reported the results removing problematic regions.

performance (F1 score of 0.64) when comparing our maps to modeled raster data, despite high agreement with government statistics, which also indicates potential errors in the construction of the raster reference maps.

In South Africa, it's worth noting that performance against the SANLC field points surpasses that of the South Africa SANLC 2020 map. For field points, the F1 score for sugarcane is 0.9, with precision at 0.97 and recall at 0.84. In contrast, the map exhibits an F1 score of 0.78, with precision and recall values of 0.73 and 0.83, respectively. In the US, where we have high confidence in the CDL maps and reference map years align with our mapping period, we observe good agreement with CDL sugarcane data. However, it is essential to emphasize that reference maps may not be equally reliable, potentially leading to discrepancies in performance evaluation.

5.2 Agreement with government statistics

The comparisons with government statistics are complicated by several factors, including the unknown accuracy of official numbers and the fact that they do not necessarily intend to reflect all of cropland area planted with sugarcane. Government data often reflect sugarcane harvested area for a single year, while our mapping captures total-stable sugarcane area over a four-year period. We therefore would expect our numbers to be slightly higher than government numbers, even if both datasets were perfectly accurate. Despite this disparity, we generally observe favorable agreement in most regions.

In India, particularly in Maharashtra and Karnataka, deviations from the 1:1 line are evident, with slope values of 2.3 and 2.2, respectively. Notably, in Maharashtra, the mapped area (2,702,144 ha) exceeds the government-reported area (822,407 ha) by over 230%. However, Plantix data in Maharashtra, which was adjusted for bias in class representation as described in section 2.4.1, revealed a low user's accuracy (50%). This is a warning that commission error associated with the sugarcane class was problematic.

To address this, we employed an error-adjusted estimator of area proposed by Olofsson et al. (2013) to correct the estimated sugarcane area and provide confidence intervals. Taking into account the presence of false positives, consisting of 955 instances among 1,911 sugarcane labels, and false negatives, comprising 529 instances among 13,384 non-sugarcane labels, alongside a proportion of area mapped as sugarcane equal to 0.15, our analysis yielded a revised estimate of sugarcane area of 1,953,625 ha. This revised estimate notably surpasses the reported area by approximately 140%.

The resulting confidence interval, computed using the method suggested by Olofsson et al. (2013), suggests that the sugarcane area estimate could range from 1,873,290 ha to 2,033,960 ha at a 95% confidence level. Despite the wide confidence interval, it is still well above the government-reported area, and the gap is too large to be explained by the difference between total and harvested area. We therefore suggest that the official numbers in Maharashtra are significantly underestimating the actual sugarcane area. This conclusion is similar to that reached in a previous study in the Upper Bhima Basin within Maharashtra, which concluded that actual sugarcane area may be twice as large as what is indicated in government statistics (Lee et al., 2022).

5.3 Future improvements

A number of future directions could improve the accuracy of our maps. A key dependency in our approach is the use of existing crop maps that delineate arable cropland from other land uses, including permanent tree crops and perennial woody crops like bamboo. Yet we observed in several regions, most notably in Southern China, that the crop mask often included areas with orchards. Because orchards are tall throughout the year, removing them from the crop mask is an important need for further improvement. Likewise, in some regions the crop masks we utilized miss some areas that appear in other sugarcane reference maps (e.g. in South Africa, see Fig. 6). By improving the accuracy of the crop mask, more precise sugarcane maps can be generated, providing more reliable information for agricultural planning and management. Implementing subnational thresholds could further refine the accuracy of our estimations, considering the localized variations in sugarcane cultivation practices. Integration of other sensor data, such as Sentinel-1, as well as other approaches to summarizing time series than the harmonic regressions used here, could enhance model performance.

In future iterations, extending the grid to encompass more geographical areas could provide a broader perspective on sugarcane dynamics. Additionally, another interesting direction for future research would be to extend our maps back in time. This would allow us to examine changes over time, observe the impact of climate change on sugarcane plantations in various regions, and provide valuable insights into temporal trends.

6 Conclusions

In this study we have introduced a dataset of sugarcane maps for the top 13 producing countries, covering nearly 90% of global production, leveraging satellite remote sensing data from GEDI and Sentinel-2 for the years 2019-2022.

Sugarcane cultivation stands as a vital economic activity globally, contributing significantly to food and biofuel production. With a quarter of the world's ethanol production sourced from sugarcane, countries like Brazil and India are positioned to substantially increase their ethanol output. However, alongside its economic benefits, sugarcane cultivation presents numerous social and environmental challenges, including water scarcity, soil pollution, and labor exploitation. Despite its pivotal role in economies worldwide, reliable information on sugarcane cultivation remains scarce.

Our methodology overcomes limitations of traditional ground-based data collection, offering a scalable approach to mapping sugarcane canopies globally. Through comparisons with field data, pre-existing maps, and government statistics, we have demonstrated the accuracy and reliability of our maps.

However, challenges persist, particularly in regions where tall crops like cassava and maize coexist with sugarcane. Additionally, our approach's dependency on existing crop maps to delineate arable cropland from other land uses presents another hurdle. These challenges underscore the necessity for ongoing refinement of our mapping techniques.

The final maps should be useful in studying the socio-economic and environmental impacts of sugarcane cultivation and producing maps of related outcomes such as sugarcane yields.

Data availability statement

The final output of our study comprises the frequency of tall mappings for each 10 by 10 m pixel in the combined crop mask (union of ESA, ESARI and GLAD), alongside the sugarcane maps for each country obtained applying the calibration threshold and the crop masks used. Results were provided for each region using the calibration threshold and masking maps using the union of the ESA and GLAD crop masks. However, with the dataset provided, users have the flexibility to use a region-specific crop mask and their own region-specific thresholds if they possess additional insight or calibration data, allowing for customization of the sugarcane mapping process.

The dataset can be accessed on Google Earth Engine at https://code.earthengine.google.com/?asset=projects/lobell-lab/gedi_sugarcane/maps/imgColl_10m_ESAESRIGLAD. Additionally, users can find the dataset on Zenodo, at https://doi.org/10.5281/zenodo.10871164 (Di Tommaso et al., 2024). In the Zenodo repository, users will also find a link to a GEE script for visualizing and masking the sugarcane maps by country.

Author contributions

SD, SW and DL designed the research. SD developed the model code and performed the analysis. SD prepared the manuscript with contributions from all co-authors.

Competing interests

The authors declare that they have no conflict of interest.

Acknowledgements

We thank Yuan Wenping for sharing the China sugarcane map, and the Google Earth Engine team for making large-scale computational resources available to researchers.

This work was supported by the NASA Harvest Consortium (NASA Applied Sciences Grant No. 80NSSC17K0652, sub-award 54308-Z6059203 to DBL).

References

Agri-Food And Fisheries Information Service: Mexico Statistical Yearbook of Agricultural Production, Available online: https://www.gob.mx/siap (accessed: February 8, 2024).

Agriculture and Agri-Food Canada: Annual Crop Inventory, Available online: https://open.canada.ca/data/en/dataset/ba2645d5-4458-414d-b196-6303ac06c1c9 (accessed: February 26, 2024).

Allan, H. L., van de Merwe, J. P., Finlayson, K. A., O'Brien, J. W., Mueller, J. F., and Leusch, F. D. L.: Analysis of sugarcane herbicides in marine turtle nesting areas and assessment of risk using *in vitro* toxicity assays, Chemosphere, 185, 656–664, https://doi.org/10.1016/j.chemosphere.2017.07.029, 2017.

Australian Bureau of Statistics: Agricultural Commodities, Australia, Available online: https://www.abs.gov.au (accessed: February 8, 2024).

Badan Pusat Statistik (BPS): Indonesia Plantation Area by Province 2021, Available online: https://www.bps.go.id/ (accessed: February 15, 2024).

Boryan, C., Yang, Z., Mueller, R., and Craig, M.: Monitoring US agriculture: the US Department of Agriculture, National Agricultural Statistics Service, Cropland Data Layer Program, Geocarto International, 26, 341–358, https://doi.org/10.1080/10106049.2011.562309, 2011.

Di Tommaso, S., Wang, S., and Lobell, D. B.: Combining GEDI and Sentinel-2 for wall-to-wall mapping of tall and short crops, Environmental Research Letters, 16, 125 002, 2021.

Di Tommaso, S., Wang, S., Vajipey, V., Gorelick, N., Strey, R., and Lobell, D. B.: Annual Field-Scale Maps of Tall and Short Crops at the Global Scale Using GEDI and Sentinel-2, Remote Sensing, 15, 4123, https://doi.org/10.3390/rs15174123, number: 17 Publisher: Multidisciplinary Digital Publishing Institute, 2023.

Di Tommaso, S., Wang, S., Strey, R., and Lobell, D. B.: Mapping Sugarcane Globally at 10 m Resolution Using GEDI and Sentinel-2, https://doi.org/10.5281/zenodo.10871164, 2024.

Dubayah, R., Blair, J. B., Goetz, S., Fatoyinbo, L., Hansen, M., Healey, S., Hofton, M., Hurtt, G., Kellner, J., Luthcke, S., Armston, J., Tang, H., Duncanson, L., Hancock, S., Jantz, P., Marselis, S., Patterson, P. L., Qi, W., and Silva, C.: The Global Ecosystem Dynamics Investigation: High-resolution laser ranging of the Earth's forests and topography, Science of Remote Sensing, 1, 100 002, 2020.

El Chami, D., Daccache, A., and El Moujabber, M.: What are the impacts of sugarcane production on ecosystem services and human well-being? A review, Annals of Agricultural Sciences, 65, 188–199, https://doi.org/10.1016/j.aoas.2020.10.001, 2020.

Food and Agriculture Organization's Statistical Database (FAOSTAT): Country-Wise Sugarcane Area and Production Data, 2022, Available online: https://www.fao.org/faostat/en/#data/QCL (accessed: February 16, 2024).

Gitelson, A. A., Vina, A., Ciganda, V., Rundquist, D. C., and Arkebauer, T. J.: Remote estimation of canopy chlorophyll content in crops, Geophysical Research Letters, 32, https://doi.org/10.1029/2005GL022688, 2005.

Gorelick, N., Hancher, M., Dixon, M., Ilyushchenko, S., Thau, D., and Moore, R.: Google Earth Engine: Planetary-scale geospatial analysis for everyone, Remote sensing of Environment, 202, 18–27, 2017.

Guangdong Provincial Bureau of Statistics: Guangdong Statistical Yearbook, Available online: http://stats.gd.gov.cn/gdtjnj/index.html (accessed: February 8, 2024).

Guatemala Nationl Institue of Statistics: National Agricultural Census 2002-2003 - Volume III, Available online: https://www.ine.gob.gt/ (accessed: February 16, 2024).

559 Hainan Provincial Bureau of Statistics: Hainan Statistical Yearbook, Available online: https://stats.hainan.gov.cn/ (accessed: February 8,
560   2024).

561 Healey, S. P., Yang, Z., Gorelick, N., and Ilyushchenko, S.: Highly local model calibration with a new GEDI LiDAR asset on Google Earth
562   Engine reduces landsat forest height signal saturation, Remote Sensing, 12, 2840, 2020.

563 Indian Department of Agriculture: Ministry of Agriculture and Farmers' Welfare, Crop Production Statistics Information System, Available
564   online: https://aps.dac.gov.in/APY/Index.htm (accessed: August 8, 2023).

565 Instituto Brasileiro de Geografia e Estatística: IBGE, Available online: https://www.ibge.gov.br/ (accessed: November 15, 2023).

566 International Food Policy Research Institute: Global Spatially-Disaggregated Crop Production Statistics Data for 2010 Version 2.0,
567   https://doi.org/10.7910/DVN/PRFF8V, 2019.

568 Jenkins, B., Baptista, P., and Porth, M.: Collaborating for Change in Sugar Production: Building blocks for sustainability at scale, 2015.

569 Karra, K., Kontgis, C., Statman-Weil, Z., Mazzariello, J. C., Mathis, M., and Brumby, S. P.: Global land use/land cover with Sentinel 2 and
570   deep learning, in: 2021 IEEE international geoscience and remote sensing symposium IGARSS, pp. 4704–4707, IEEE, 2021.

571 Kerner, H., Nakalembe, C., Yang, A., Zvonkov, I., McWeeny, R., Tseng, G., and Becker-Reshef, I.: How accurate are existing land cover
572   maps for agriculture in Sub-Saharan Africa?, 2023.

573 Laguarta, J., Friedel, T., and Wang, S.: Combining deep learning and street view imagery to map smallholder crop types, http://arxiv.org/abs/
574   2309.05930, arXiv:2309.05930 [cs], 2023.

575 Lee, J. Y., Naylor, R. L., Figueroa, A. J., and Gorelick, S. M.: Water-food-energy challenges in India: political economy of the sugar industry,
576   Environmental Research Letters, 15, 084 020, https://doi.org/10.1088/1748-9326/ab9925, publisher: IOP Publishing, 2020.

577 Lee, J. Y., Wang, S., Figueroa, A. J., Strey, R., Lobell, D. B., Naylor, R. L., and Gorelick, S. M.: Mapping Sugarcane in Central India with
578   Smartphone Crowdsourcing, Remote Sensing, 14, 703, 2022.

579 Lesiv, M., Bilous, A., Bayas, J. C. L., Karanam, S., and Fritz, S.: Global Crop Type Validation Data Set for ESA WorldCereal System,
580   https://doi.org/10.5281/zenodo.7825628, 2023.

581 Ministry of National Food Security and Research: Pakistan Government statistics, Available online: https://mnfsr.gov.pk (accessed: Septem-
582   ber 28, 2023).

583 National Administrative Statistics Department: DANE National agricultural survey, Available online: https://www.dane.gov.co (accessed:
584   February 14, 2024).

585 OECD: Agricultural Policy Monitoring and Evaluation 2023, https://doi.org/10.1787/b14de474-en, 2023.

586 OECD, Food, and of the United Nations, A. O.: OECD-FAO Agricultural Outlook 2023-2032, https://doi.org/10.1787/08801ab7-en, 2023.

587 Office of Agricultural Economics: Thailand Statistical Yearbook, Available online: https://www.oae.go.th/ (accessed: January 18, 2024).

588 Olofsson, P., Foody, G. M., Stehman, S. V., and Woodcock, C. E.: Making better use of accuracy data in land change studies: Es-
589   timating accuracy and area and quantifying uncertainty using stratified estimation, Remote Sensing of Environment, 129, 122–131,
590   https://doi.org/10.1016/j.rse.2012.10.031, 2013.

591 Philippine Statistics Authority: Philippines Selected Statistics on Agriculture and Fisheries, Available online: https://psa.gov.ph/ (accessed:
592   February 13, 2024).

593 Potapov, P., Turubanova, S., Hansen, M. C., Tyukavina, A., Zalles, V., Khan, A., Song, X.-P., Pickens, A., Shen, Q., and Cortez, J.:
594   Global maps of cropland extent and change show accelerated cropland expansion in the twenty-first century, Nature Food, 3, 19–28,
595   https://doi.org/10.1038/s43016-021-00429-z, number: 1 Publisher: Nature Publishing Group, 2022.

Roy, S., Swetnam, T., Robitaille, A., Trochim, E., and Pasquarella, V.: samapriya/awesome-gee-community-datasets: Community Catalog (1.0.1). Available at https://doi.org/10.5281/zenodo.7271726 (accessed 2024-02-02), 2024.

South Africa - DFFE: South African National Landcover Data (SANLC) 2020, Available online: https://egis.environment.gov.za/gis_data_downloads (accessed: August 1, 2023).

Statistics Bureau of Guangxi Zhuang Autonomous Region: Guangxi Statistical Yearbook, Available online: http://tjj.gxzf.gov.cn/ (accessed: February 8, 2024).

Statistics Department - South Africa: Census of commercial agriculture, 2017, Available online: https://www.statssa.gov.za/ (accessed: February 16, 2024).

USDA Natlional Agricultural Statistics Service: NASS Quick Stats API, Available online: https://www.nass.usda.gov/ (accessed: February 1, 2024).

Wang, S., Di Tommaso, S., Faulkner, J., Friedel, T., Kennepohl, A., Strey, R., and Lobell, D. B.: Mapping Crop Types in Southeast India with Smartphone Crowdsourcing and Deep Learning, Remote Sensing, 12, 2020.

Yunnan Provincial Bureau of Statistics: Yunnan Statistical Yearbook, Available online: https://stats.yn.gov.cn/ (accessed: February 8, 2024).

Zanaga, D., Van De Kerchove, R., De Keersmaecker, W., Souverijns, N., Brockmann, C., Quast, R., Wevers, J., Grosu, A., Paccini, A., Vergnaud, S., et al.: ESA WorldCover 10 m 2020 v100, Zenodo: Geneve, Switzerland, 2021.

Zheng, Y., dos Santos Luciano, A. C., Dong, J., and Yuan, W.: High-resolution map of sugarcane cultivation in Brazil using a phenology-based method, Earth System Science Data, 14, 2065–2080, https://doi.org/10.5194/essd-14-2065-2022, 2022a.

Zheng, Y., Li, Z., Pan, B., Lin, S., Dong, J., Li, X., and Yuan, W.: Development of a Phenology-Based Method for Identifying Sugarcane Plantation Areas in China Using High-Resolution Satellite Datasets, Remote Sensing, 14, 1274, https://doi.org/10.3390/rs14051274, number: 5 Publisher: Multidisciplinary Digital Publishing Institute, 2022b.